Surfactant-Free, Large-Scale, Solution−Liquid−Solid Growth of Gallium Phosphide Nanowires and Their Use for Visible-Light-Driven Hydrogen Production from Water Reduction

Jianwei Sun,[†,‡] Chong Liu,[‡] and Peidong Yang*[,†,‡]

[†]Joint Center for Artificial Photosynthesis (JCAP), Lawrence Berkeley National Laboratory, Berkeley, California 94720, United States
[‡]Department of Chemistry, University of California, Berkeley, California 94720, United States

S *Supporting Information*

ABSTRACT: Colloidal GaP nanowires (NWs) were synthesized on a large scale by a surfactant-free, self-seeded solution−liquid−solid (SLS) method using triethylgallium and tris(trimethylsilyl)phosphine as precursors and a noncoordinating squalane solvent. Ga nanoscale droplets were generated in situ by thermal decomposition of the Ga precursor and subsequently promoted the NW growth. The GaP NWs were not intentionally doped and showed a positive open-circuit photovoltage based on photoelectrochemical measurements. Purified GaP NWs were used for visible-light-driven water splitting. Upon photodeposition of Pt nanoparticles on the wire surfaces, significantly enhanced hydrogen production was observed. The results indicate that colloidal surfactant-free GaP NWs combined with potent surface electrocatalysts could serve as promising photocathodes for artificial photosynthesis.

Solar energy is, among various renewable energy sources, the largest energy source that would ultimately solve the terawatt energy challenge.[1] Because of its intermittency and daily and seasonal variation, solar energy must be captured, converted, and stored for use upon demand. Storing solar energy directly in high-energy chemical bonds, such as solar water splitting to hydrogen and oxygen, is one of the most attractive approaches.[2] A single semiconductor may be used to achieve overall solar water splitting. However, because of the large overpotentials associated with the sluggish multielectron-transfer kinetics at semiconductor−electrolyte interfaces, this generally requires semiconductors having large band gaps that poorly match the solar spectrum, resulting in low efficiency.[3] This problem may be overcome by using two small-band-gap semiconductors having a Z-scheme configuration (i.e., one as the photocathode for hydrogen evolution and the other as the photoanode for oxygen evolution), which closely mimics nature's photosynthesis.[4]

Because its conduction-band edge is ∼1 V more negative than both the standard water and CO_2 reduction potentials and its band gap is relatively small (2.27 eV at 300 K), GaP is one of the most promising photocathode materials for water and CO_2 reduction. The first use of GaP as a photocathode for visible-light-driven water reduction was reported more than three decades ago.[5] Roughly at the same time, overall solar water splitting at zero bias was demonstrated using Z-scheme photoelectrochemical (PEC) cells composed of a p-type GaP photocathode and a suitable n-type metal oxide photoanode.[6] These early studies all used low-surface-area bulk materials.

The utilization of one-dimensional semiconductor micro- and nanowires (NWs) for solar water splitting has recently attracted growing attention.[7] In comparison with bulk materials, single-crystalline NWs are advantageous for solar-to-fuel conversion because the reduced radial dimension and the increased surface-to-volume ratio facilitate rapid diffusion of photogenerated charge carriers to the NW surfaces, which can be decorated with high-surface-area catalysts to perform the desired chemistry.[8] To date, the synthesis of GaP NWs has been dominated by high-temperature vapor-phase approaches.[9] Solution-based syntheses of colloidal NWs may be readily scaled up to produce grams of product[10] but often require the use of organic surfactants/ligands to achieve the desired morphology control.[11] Because the covalently bound surface organic molecules generally prevent efficient injection of photogenerated carriers to electrolytes, additional efforts to remove them are necessary before the NWs can be used for solar water splitting. Herein we report a *surfactant-free*, self-seeded solution−liquid−solid (SLS)[12] approach for growing high-quality GaP NWs on a large scale. This is the first time that colloidal semiconductor NWs have been grown by an SLS method in the absence of surfactants/ligands. With these GaP NWs having clean surfaces, we have been able to demonstrate their great potential as visible-light-responsive photocathodes for artificial photosynthesis.
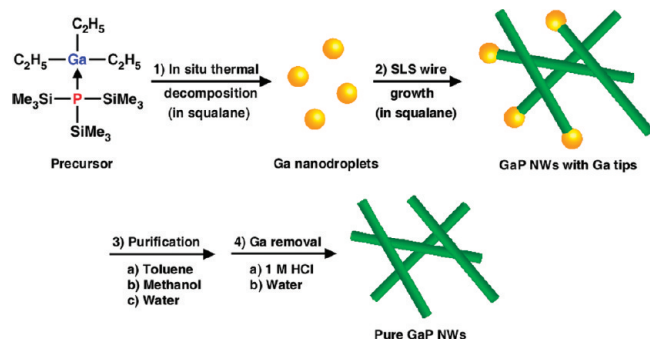
Our SLS syntheses of GaP NWs used triethylgallium (TEG) and tris(trimethylsilyl)phosphine (TMSP) as precursors. In addition, we used saturated hydrocarbons having high boiling points as solvents to synthesize straight GaP NWs. Squalane was empirically found to be the best solvent, which is likely due to its noncoordinating nature and high viscosity. The wire growth in squalane was found to be a self-seeded SLS process: the precursor first thermally decomposes in situ to generate nanoscale Ga droplets, which then subsequently promote the growth of GaP NWs via the SLS mechanism (Scheme 1).

In the absence of surface ligands, small Ga nanodroplets tend to grow rapidly and aggregate, resulting in highly tapered wires [Figure S1 in the Supporting Information (SI)]. To achieve better control over the wire growth, we optimized the synthetic

Scheme 1. Synthesis and Purification of Colloidal GaP Nano-wires: The NWs Are Grown in Squalane Using a Surfactant-Free, Self-Seeded, Solution−Liquid−Solid (SLS) Method

conditions, including the precursor ratio, concentration, and stirring. In a typical synthesis (for experimental details, see the SI), the Ga and P precursors (1:1 molar ratio) were quickly injected into hot squalane solvent at 290 °C. The mixture was vigorously stirred for 30 s to form a homogeneous solution. After the stirring was stopped, the color of the solution changed to yellow in 15−20 s as a result of the generation of Ga nanodroplets and then quickly to dark-brown as the NWs grew. We note that although the initial precursor ratio was 1:1, the P precursor was in slight excess during wire growth because a portion of the Ga precursor was first consumed to generate the Ga nanoparticles (NPs). The product yield reached ∼80% under the optimized conditions.

Representative low- and high-magnification transmission electron microscopy (TEM) images of the as-synthesized GaP NWs showed that the wires were relatively uniform with lengths of 1−2 μm (Figure 1a) and diameters of ∼30 nm (Figure 1b). A detailed TEM study showed that the wires were slightly tapered at the NP-free end (Figure S2), indicating that the initially generated Ga NPs grew during the wire growth until a steady state was achieved. The single-crystalline nature of the NWs was clearly seen in a lattice-resolved high-resolution TEM (HRTEM) image (Figure 1c). The fast Fourier transform (FFT) pattern of the image was indexed to the zinc blende structure (Figure 1c inset) and indicated a wire growth in the [111] direction. The spacing of the lattice fringes perpendicular to the growth direction was measured to be 0.316 nm, consistent with the d spacing of (111) planes in zinc blende GaP. The zinc blende structure of the GaP NWs was also confirmed by powder X-ray diffraction (XRD) (Figure 1e).

To remove the viscous squalane solvent and any unreacted precursors and byproducts, the as-synthesized GaP NWs were thoroughly washed with toluene, methanol, and deionized water in sequence. The purified wires could be readily dispersed in aqueous solutions. We next sought to remove the Ga NPs attached to NW tips effectively without damage to the wires. Since Ga reacts with hydrochloric acid ($2Ga + 6HCl \rightarrow 2GaCl_3 + 3H_2$) while GaP does not,[13] the purified GaP NWs were then dispersed in 1 M HCl with stirring. Bubbles due to the formation of hydrogen gas were observed. A TEM image recorded after the HCl treatment (Figure 1d) showed that all of the Ga NPs were completely etched away, and no change in the diameter of the NWs was noticed.

Our surfactant-free synthesis of GaP NWs can be easily scaled up. To demonstrate this, ∼75 mg of purified, Ga-removed wires were prepared using 300 mL of squalane according to the general procedure described above and in Scheme 1. A large NW membrane
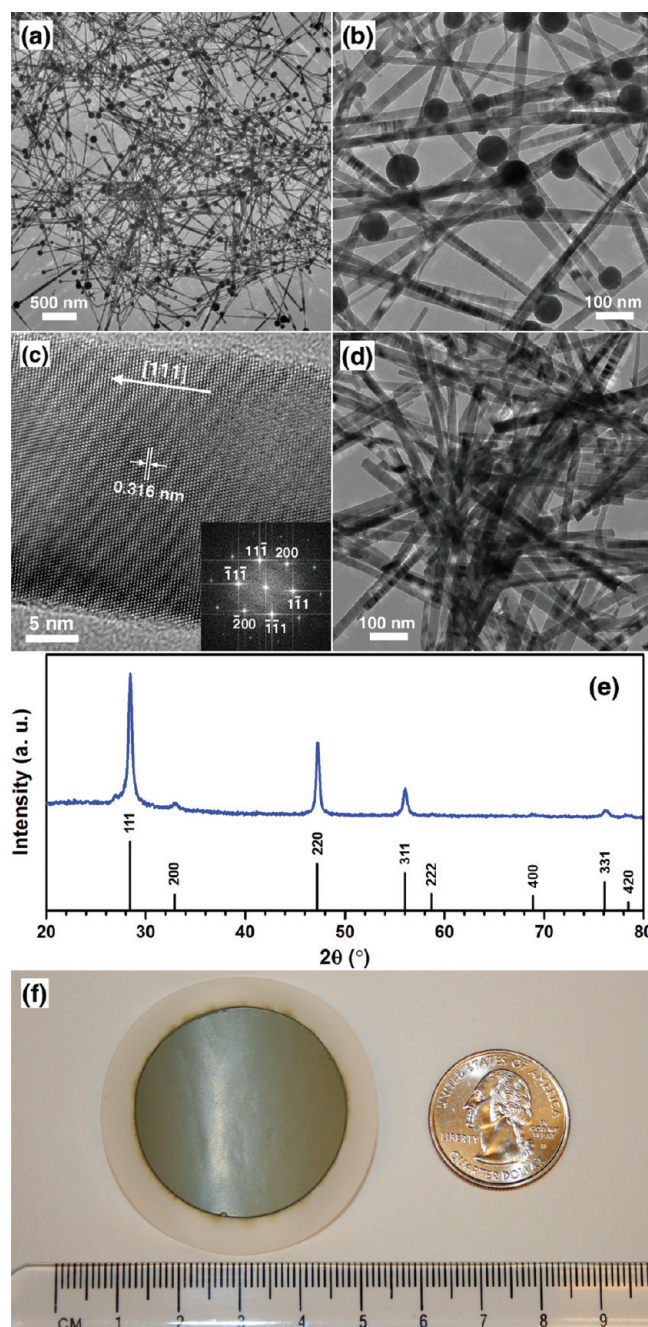
Figure 1. GaP NWs synthesized using a surfactant-free, self-seeded SLS method. (a, b) Low- and high-magnification TEM images of as-prepared wires. (c) HRTEM image of a single nanowire; the inset shows the indexed FFT pattern of the image, indicating that the wire grows along the [111] direction. (d) TEM image of GaP nanowires after treatment in 1 M hydrochloric acid solution. (e) XRD pattern of GaP nanowires (blue); the standard pattern of zinc blende GaP (black bars; JCPDS no. 12-0191) is also shown for comparison. (f) Photograph of a large GaP nanowire membrane on a PVDF filter membrane (white); the quarter-dollar coin in the image is for comparison.

(Figure 1f) was then made by filtration of an aqueous NW suspension through a commercial poly(vinylidene fluoride) (PVDF) filter membrane.

The UV−vis absorption spectrum collected from an aqueous suspension of purified, Ga-removed GaP NWs (Figure 2a) showed
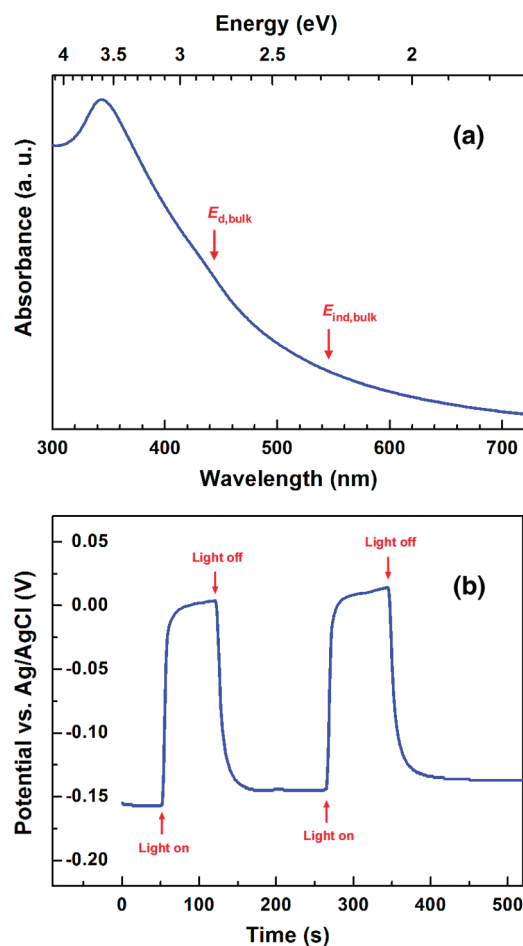
Figure 2. (a) UV−vis absorption spectrum of purified, Ga-removed GaP NWs dispersed in water. The indirect ($E_{ind,bulk}$) and direct ($E_{d,bulk}$) energy gaps of bulk GaP are indicated by red arrows. (b) Photoelectrochemical open-circuit photovoltage measurements on a GaP NW photoelectrode, showing a positive open-circuit photovoltage. The measurement was conducted using simulated AM1.5 illumination (1 sun).

Figure 3. GaP nanowires for hydrogen production under visible-light illumination. (a) Hydrogen evolution as a function of illumination time for both unloaded and Pt-loaded (2 wt %) wires (1 mg) dispersed in methanol/water solution (1:5 by volume, 3 mL). The visible light was obtained by placing a 400 nm long-pass filter in front of a 450 W Xe lamp. (b) HRTEM image of a Pt-loaded (5 wt %) GaP NW. (c, d) HRTEM images of GaP NWs (c) before and (d) after visible-light illumination for 18 h.

that the wires absorb photons in the visible region, consistent with the direct energy gap of bulk GaP (2.79 eV at 298 K[14]) and the indirect band gap at 2.3 eV. We note that light scattering from the suspended wires is obvious in the spectrum, indicated by the extended tail to the near-IR region.

We next studied the PEC performance of GaP NW photoelectrodes fabricated by drop-casting GaP NWs suspended in acetone onto an Au/Zn/Au-coated glass substrate. To achieve good contact between the NWs and the substrate, the as-made photoelectrodes were annealed in Ar for 1 h at 200 °C. Before the PEC measurements, the NW electrodes were freshly etched to remove surface oxide. An open-circuit photovoltage measurement in 0.1 M acetate buffer solution (pH 5.2) using simulated AM1.5 1 sun illumination showed that the NW photoelectrode exhibited ∼0.15 V more positive potential in the light than in the dark (Figure 2b). We note that consistent results were obtained using various contacts such as Cr−Au and In−indium tin oxide, indicating that the positive open-circuit photovoltage behavior is intrinsic to the GaP NW−electrolyte interface. We also note that the small drift of the plateau potentials is likely due to slow oxidation of the NW surfaces in the aqueous electrolyte under the open-circuit conditions.
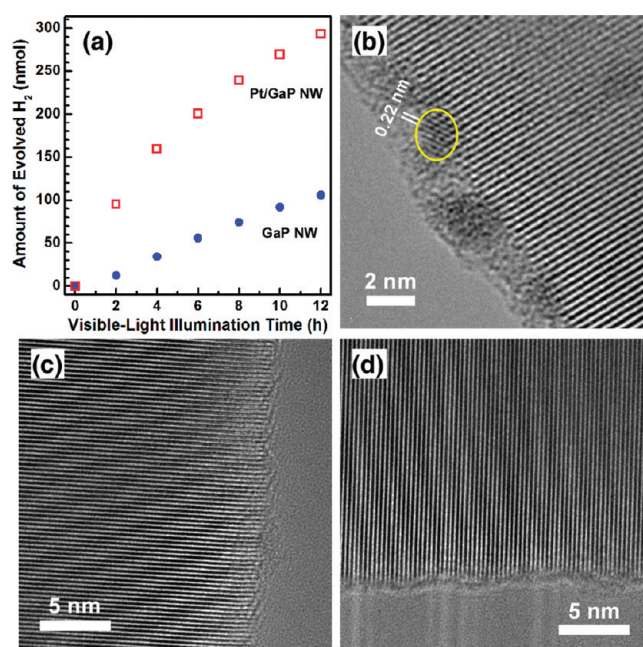
The capability of our GaP NWs to drive hydrogen evolution from water reduction under visible-light illumination at neutral pH was demonstrated by gas chromatography (GC) (Figure 3a). Methanol was used as a hole scavenger. With 1 mg of GaP wires, hydrogen was produced at a rate of ∼9 nmol/h. In a control experiment conducted in the absence of NWs, hydrogen was not detected. HRTEM images before (Figure 3c) and after (Figure 3d) 18 h GC measurement under continuous illumination confirmed that there was no noticeable change in the wire surfaces, indicating that our GaP NWs are stable under the GC measurement conditions investigated.

It is well-known that surface-bound electrocatalysts can significantly improve the water-splitting performance of semiconductors.[2b] As a proof-of-concept, we photochemically deposited small Pt NPs onto the GaP NW surfaces using H_2PtCl_6 precursor dissolved in a methanol/water solution. The size of the deposited Pt NPs was found to be related to the Pt loading amount (determined by the initial H_2PtCl_6/NW ratio) under fixed illumination conditions. Higher Pt loadings yielded relatively larger Pt NPs. The HRTEM image of a GaP NW with 5 wt % Pt loading (Figure 3b) showed 1−2 nm NPs anchored on the surface of a single wire. The spacing of the lattice fringes in a lattice-resolved NP was measured to be 0.22 nm, consistent with the d spacing of the (111) planes in cubic Pt. When the Pt loading was reduced to 2 wt %, the deposited NPs could not be clearly imaged by TEM. However, Pt signals were detected by X-ray photoelectron spectroscopy (XPS) (Figure S3), suggesting that only extremely small Pt clusters (<1 nm) were deposited at low Pt loadings. GC measurements were also conducted using these Pt-loaded GaP NWs under the same conditions used for the

19308

dx.doi.org/10.1021/ja2083398 |*J. Am. Chem. Soc.* 2011, 133, 19306–19309

parent unloaded GaP NWs described above. The hydrogen production rate of the Pt-loaded GaP NWs at a low Pt loading of 2 wt % was ∼1 order of magnitude higher than that of the parent wires during the first 2 h (Figure 3a), indicating significantly enhanced water reduction activity. We note that the Pt-loaded wires tended to gradually accumulate to the top of the electrolyte at longer reaction times, resulting in an apparent decrease of the hydrogen production rate. More systematic studies of GaP NWs decorated with various water-reduction electrocatalysts are currently underway.

In summary, surfactant-free SLS growth of semiconducting GaP NWs has been demonstrated for the first time. The wire growth is catalyzed by in situ-generated Ga nanodroplets, which can be effectively removed by selective etching using hydrochloric acid. Purified, Ga-removed NWs exhibited a positive open-circuit photovoltage and were able to drive hydrogen production under visible-light illumination. The hydrogen production rate was significantly enhanced upon photochemical deposition of small Pt clusters on the NW surfaces, indicating that our GaP NWs decorated with potent electrocatalysts should be promising photocathodes for artificial photosynthesis.

■ ASSOCIATED CONTENT

S **Supporting Information.**   Experimental details, additional TEM images, and XPS spectra. This material is available free of charge via the Internet at http://pubs.acs.org.

■ AUTHOR INFORMATION

Corresponding Author
p_yang@uclink.berkeley.edu

■ ACKNOWLEDGMENT

■ REFERENCES

(1) Lewis, N. S.; Nocera, D. G. *Proc. Natl. Acad. Sci. U.S.A.* **2006**, *103*, 15729–15735.

(2) (a) Bard, A. J.; Fox, M. A. *Acc. Chem. Res.* **1995**, *28*, 141–145. (b) Walter, M. G.; Warren, E. L.; McKone, J. R.; Boettcher, S. W.; Mi, Q.; Santori, E. A.; Lewis, N. S. *Chem. Rev.* **2010**, *110*, 6446–6473.

(3) Kudo, A. *Int. J. Hydrogen Energy* **2006**, *31*, 197–202.

(4) (a) Grätzel, M. *Nature* **2001**, *414*, 338–344. (b) Kudo, A. *MRS Bull.* **2011**, *36*, 32–38. (c) Bolton, J. R.; Strickler, S. J.; Connolly, J. S. *Nature* **1985**, *316*, 495–500.

(5) Tomkiewicz, M.; Woodall, J. M. *Science* **1977**, *196*, 990–991.

(6) (a) Nozik, A. J. *Appl. Phys. Lett.* **1976**, *29*, 150–153. (b) Mettee, H.; Otvos, J. W.; Calvin, M. *Sol. Energy Mater.* **1981**, *4*, 443–453.

(7) (a) Boettcher, S. W.; Warren, E. L.; Putnam, M. C.; Santori, E. A.; Turner-Evans, D.; Kelzenberg, M. D.; Walter, M. G.; McKone, J. R.; Brunschwig, B. S.; Atwater, H. A.; Lewis, N. S. *J. Am. Chem. Soc.* **2011**, *133*, 1216–1219. (b) Hwang, Y. J.; Boukai, A.; Yang, P. *Nano Lett.* **2009**, *9*, 410–415. (c) Liu, M.; de Leon Snapp, N.; Park, H. *Chem. Sci.* **2011**, *2*, 80–87. (d) Wang, G.; Wang, H.; Ling, Y.; Tang, Y.; Yang, X.; Fitzmorris, R. C.; Wang, C.; Zhang, J. Z.; Li, Y. *Nano Lett.* **2011**, *11*, 3026–3033. (e) Jitputti, J.; Suzuki, Y.; Yoshikawa, S. *Catal. Commun.* **2008**, *9*, 1265–1271. (f) Yang, X.; Wolcott, A.; Wang, G.; Sobo, A.; Fitzmorris, R. C.; Qian, F.; Zhang, J. Z.; Li, Y. *Nano Lett.* **2009**,

9, 2331–2336. (g) Chakrapani, V.; Thangala, J.; Sunkara, M. K. *Int. J. Hydrogen Energy* **2009**, *34*, 9050–9059. (h) Su, J.; Feng, X.; Sloppy, J. D.; Guo, L.; Grimes, C. A. *Nano Lett.* **2011**, *11*, 203–208.

(8) (a) Hochbaum, A. I.; Yang, P. *Chem. Rev.* **2010**, *110*, 527–546. (b) Yang, P.; Yan, R.; Fardy, M. *Nano Lett.* **2010**, *10*, 1529–1536.

(9) (a) Duan, X.; Lieber, C. M. *Adv. Mater.* **2000**, *12*, 298–302. (b) Seo, H. W.; Bae, S. Y.; Park, J.; Yang, H.; Kim, S. *Chem. Commun.* **2002**, 2564–2565. (c) Borgstrom, M. T.; Immink, G.; Ketelaars, B.; Algra, R.; BakkersErik, P. A. M. *Nat. Nanotechnol.* **2007**, *2*, 541–544. (d) Lyu, S. C.; Zhang, Y.; Ruh, H.; Lee, H. J.; Lee, C. J. *Chem. Phys. Lett.* **2003**, *367*, 717–722. (e) Gu, Z.; Paranthaman, M. P.; Pan, Z. *Cryst. Growth Des.* **2009**, *9*, 525–527.

(10) (a) Park, J.; An, K.; Hwang, Y.; Park, J.-G.; Noh, H.-J.; Kim, J.-Y.; Park, J.-H.; Hwang, N.-M.; Hyeon, T. *Nat. Mater.* **2004**, *3*, 891–895. (b) Li, J. J.; Wang, Y. A.; Guo, W.; Keay, J. C.; Mishima, T. D.; Johnson, M. B.; Peng, X. *J. Am. Chem. Soc.* **2003**, *125*, 12567–12575. (c) Joo, J.; Kwon, S. G.; Yu, T.; Cho, M.; Lee, J.; Yoon, J.; Hyeon, T. *J. Phys. Chem. B* **2005**, *109*, 15297–15302.

(11) (a) Yin, Y.; Alivisatos, A. P. *Nature* **2005**, *437*, 664–670. (b) Xiong, Y.; Xie, Y.; Li, Z.; Li, X.; Gao, S. *Chem.—Eur. J.* **2004**, *10*, 654–660. (c) Yang, Q.; Tang, K.; Li, Q.; Yin, H.; Wang, C.; Qian, Y. *Nanotechnology* **2004**, *15*, 918–922. (d) Fanfair, D. D.; Korgel, B. A. *Cryst. Growth Des.* **2005**, *5*, 1971–1976. (e) Davidson, F. M., III; Wiacek, R.; Korgel, B. A. *Chem. Mater.* **2005**, *17*, 230–233. (f) Liu, Z.; Sun, K.; Jian, W.-B.; Xu, D.; Lin, Y.-F.; Fang, J. *Chem.—Eur. J.* **2009**, *15*, 4546–4552.

(12) (a) Trentler, T. J.; Hickman, K. M.; Goel, S. C.; Viano, A. M.; Gibbons, P. C.; Buhro, W. E. *Science* **1995**, *270*, 1791–1794. (b) Wang, F.; Dong, A.; Sun, J.; Tang, R.; Yu, H.; Buhro, W. E. *Inorg. Chem.* **2006**, *45*, 7511–7521.

(13) Ellis, W. C.; Frosch, C. J.; Zetterstrom, R. B. *J. Cryst. Growth* **1968**, *2*, 61–68.

(14) Madelung, O. *Semiconductors: Data Handbook*, 3rd ed.; Springer: Berlin, 2004.